Instabilities of cylindrical bubble clusters

K.A. Brakke[1,a] and F. Morgan[2,b]

[1] Mathematics Department, Susquehanna University, Selinsgrove, PA 17870, USA
[2] Department of Mathematics and Statistics, Williams College, Williamstown, MA 01267, USA

Abstract. Small bubbles in an experimental two-dimensional foam between glass plates regularly undergo a three-dimensional instability as the small bubbles shrink under diffusion or equivalently as the plate separation increases, and end up on one of the plates. The most recent experiments of Cox, Weaire, and Vaz are accompanied by Surface Evolver computer simulations and rough theoretical calculations. We show how a recent second variation formula may be used to perform exact theoretical calculations for infinitesimal perturbations for such a system, and verify results with Surface Evolver simulations.

PACS. 82.70.Rr Aerosols and foams – 47.20.Dr Surface-tension-driven instability

1 Introduction

Experiments with two-dimensional soap films, as between two wet, parallel glass plates (see [1] and references therein), exhibit three-dimensional instabilities, in which small bubbles fatten at one plate and shrink at the other, eventually moving entirely to one plate. The simplest example is a variant of the classical Rayleigh-Plateau instability, in which a cylindrical soap bubble of decreasing volume V between two plates at increasing separation H becomes unstable (without gas exchange or further changes of volume) when $H = \sqrt[3]{\pi V} \approx 1.46\sqrt[3]{V}$ and ultimately deforms to a hemisphere on one plate ([2,3]). Cox, Weaire, and Vaz [1] considered such "wine-bottle" instabilities for cylindrical bubble clusters consisting of a central bubble surrounded by N "petal" bubbles, as in Figure 1. Inspired by their experiments, simulations, and rough theoretical computations, we use the recent exact second variation formula of [4] for an accurate theoretical computation of such instabilities for infinitesimal perturbations. We also make a small correction to one of the formulas of [1] (see our *Remark 1*).

There are three modes of instability that affect different parameter ranges:

1) A central Rayleigh-Plateau instability, in which the central bubble fattens at one end and shrinks at the other.

2) An alternating Rayleigh-Plateau instability of the petals, as in Figure 1. The sides of the central bubble undergo alternate expansion and contraction. This mode

must be suitably modulated for an odd number of petals; here we consider only N even.

3) An essentially two-dimensional buckling of the ring of petals, as in Figure 5 below.

Mathematica [5] was used to solve equations numerically to obtain theoretical predictions of instability. The Surface Evolver software [6] was used to verify many of the results to five significant figures and provide convincing evidence that we have found all modes of instability.

Theorem 1 – *A cylindrical bubble cluster of N identical petals of volume V_p surrounding a central bubble of volume V_c as in Figure 1 has its onset of instability at the height typified by those listed in Table 1 and shown in Figure 2.*

The proof, a computation for each mode by the second variation formula, occupies the rest of this paper, with more detailed results in Sections 5 through 8. As for the classical Rayleigh-Plateau instability, optimal variations are sinusoidal in the height, and take the form $v(t)\sin \pi z/H$, where t denotes arclength along the interfaces of the two-dimensional foam. The form of the second variation formula (Sect. 2) implies that the optimal $v(t)$ are piecewise linear or trigonometric (see *Lemmas 1-3*) and makes exact computation possible.

This paper is concerned only with the existence of unstable modes. It does not attempt to determine which may be dynamically dominant, which determination is often subsumed by the phrase "Rayleigh-Plateau instability".

Remark 1 – The rough theoretical computations of equation (8) in [1] shown in our Table 1(6) should have the cube root instead of the square root of $\frac{6}{6-n}$, yielding the

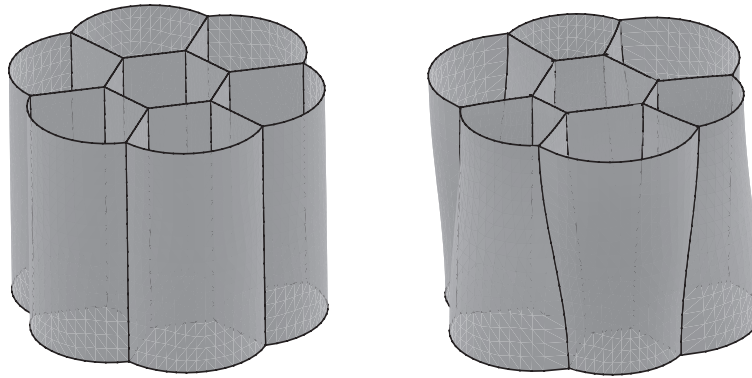ᵃ e-mail: brakke@susqu.edu
ᵇ e-mail: frank.morgan@williams.edu

Fig. 1. Symmetric cluster with $N = 6$ petals at its critical height and the petal Rayleigh mode instability.
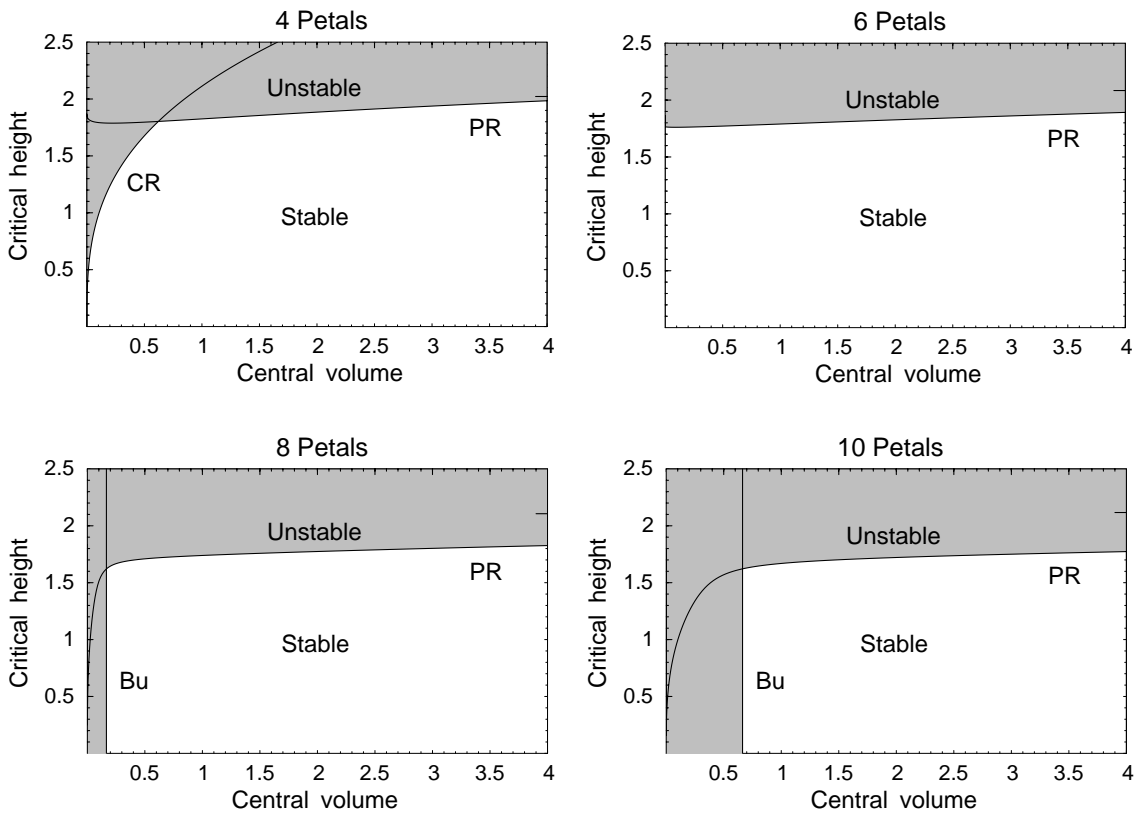

Fig. 2. Summary of instabilities for unit volume petals and varying central bubble volume. PR denotes the petal Rayleigh mode instability, CR denotes the central Rayleigh-Plateau instability, and Bu denotes petal buckling instability. The tick mark on the right edge is the critical height at the maximum central volume (where the septum length is zero), which is too large to reasonably show here. Note that for $N = 4$, petal Rayleigh mode has a small upturn as the central volume goes to zero.

improved estimates in Table 1(7), meant to be accurate only for single *symmetric* unstable bubbles, lines (a) and (c). Even then, there is a small error due to approximation in the second, tilt term of equation (2) of [1]. Our computations of column (8) do not assume such bubble symmetry. They also vary all petals simultaneously, rather than varying a single petal, the latter yielding a later instability. Similarly, equation (9) in [1] should have an exponent of 1 instead of 3/2.

2 The second variation formula

The following formula gives the second variation of area for an equilibrium bubble cluster of prescribed volumes.

Theorem 2 – *Second variation formula for equilibrium bubble clusters (Ref.* [4]*, Prop. 3.3)*

Let S be an equilibrium bubble cluster of prescribed volumes in $\mathbf{R}^3$*, possibly with free boundary along planes,*

Table 1. Comparison of previous and current results for the height of instability of cylindrical clusters of N bubbles of volume V_p surrounding a central bubble of volume V_c. Column (4) gives the Evolver simulations, column (5) the experimental results, and column (6) the rough theoretical results of [1]. Column (7) corrects for a mistake in equation (8) of [1] (see *Remark 1*). Column (8) gives results from this paper. Row (a) is classical. Row (b) is a cylinder over the classical double bubble; see Section 8. Row (c) is a central Rayleigh-Plateau instability. Rows (d)-(l) are petal Rayleigh instabilities. Petal buckling instability does not occur for six or fewer petals. Dimensions are in any consistent system of units.

	(1)	(2)	(3)	(4)	(5)	(6)	(7) cor'd	(8)
	N^1 petals	V_p	V_c	[1] sim.	[1] exp.	[1] theo.	[1] theo.	New theo.
(a)	0		1	1.47		1.46	1.46	1.46
(b)	2	1	0	1.57[2]			1.68	1.57
(c)	4	1	0.5	1.68		2.01	1.68	1.68
(d)	4	1	1	1.94		2.54	2.11	1.83
(e)	4	1	2	1.94		2.54	2.11	1.88
(f)	6	1	0.5	1.83		2.54	2.11	1.77
(g)	6	1	1	1.83		2.54	2.11	1.80
(h)	6	1	1.5	1.83		2.54	2.11	1.81
(i)	6	0.0147	0.009–0.03	0.45	0.45	0.62[3]	0.51[4]	0.44[5]
(j)	6	0.018	0.004–0.05	0.48	0.55	0.66[3]	0.55[4]	0.47[5]
(k)	6	0.047	0.008–0.12	0.66	0.65	0.92[3]	0.76[4]	0.65[5]
(l)	6	0.056	0.014–0.077	0.70	0.60	0.97[3]	0.81[4]	0.68[5]

[1] [1] use N for the total number of bubbles, our $N+1$; [2] private communication; [3] $2.54V_p^{1/3}$; [4] $2.11V_p^{1/3}$; [5] $1.80V_p^{1/3}$.

with unit normal $\mathbf{N}$. *Assume that S consists of smooth constant-mean-curvature surfaces S_i with unit normals $\mathbf{N}_i$ meeting smoothly in threes at 120 degrees along smooth curves C_j and meeting the boundary planes orthogonally. Let $\mathbf{V}$ be a smooth vector field. Then for any smooth, volume-preserving variation with initial velocity $\mathbf{V}$, the second derivative of area is initially*

$$\delta^2 A = \int\!\!\int_S |\nabla u|^2 - \sigma^2 u^2 \mathrm{d}A - \sum_j \int_{C_j} \sum_{i=1}^3 q_i u_i^2 \mathrm{d}s. \quad (1)$$

Here u is the normal component of the variation: $u = \mathbf{V} \cdot \mathbf{N}$ and $u_i = \mathbf{V} \cdot \mathbf{N}_i$, and σ^2 is the sum of the squares of the principal curvatures. The last sum is taken over the three surfaces, say S_1, S_2, S_3 (labeled and oriented, say counterclockwise), meeting along C_j, and the functions q_i are given by

$$q_1 = \frac{\kappa_3 - \kappa_2}{\sqrt{3}}, \qquad q_2 = \frac{\kappa_1 - \kappa_3}{\sqrt{3}}, \qquad q_3 = \frac{\kappa_2 - \kappa_1}{\sqrt{3}}, \quad (2)$$

where κ_i is the curvature of surface S_i in the direction perpendicular to C_j.

Remark 2 – The same formula holds for general soap bubble clusters with tetrahedral as well as triple line singularities (see [7], Chapt. 13), because the isolated singularities are negligible by the argument of [8], pp. 2332-2333. If the free boundary planes are replaced by more general C^2 hypersurfaces, the formula requires another term.

It will be convenient to use a coordinate system (t, z) on the surfaces, where z is the vertical coordinate and t

is a horizontal arclength measured from some convenient origin. The second variation formula in these variables becomes

$$\delta^2 A = \int\!\!\int u_t^2 + u_z^2 - \sigma^2 u^2 \mathrm{d}t \mathrm{d}z - \sum_j \int_{C_j} \sum_{i=1}^3 q_i u_i^2 \mathrm{d}z. \quad (3)$$

The following three standard lemmas, which we state without proof, will allow us to design each mode of instability to minimize the second variation.

Lemma 1 – *The minimum value of $\int u_t^2 \mathrm{d}t$ on an interval of length T with boundary values $u(0) = b$ and $u(T) = c$ is*

$$(b^2 + c^2 - 2bc)/T, \quad (4)$$

and occurs when $u(t)$ is linear.

Lemma 2 – *The minimum value of $\int u_t^2 - \lambda^2 u^2 \mathrm{d}t$ on an interval of length T with boundary values $u(0) = b$ and $u(T) = c$ is*

$$\lambda((b^2 + c^2)\cos(\lambda T) - 2bc)/\sin(\lambda T), \quad (5)$$

and occurs when $u(t)$ is of the form $u(t) = A\cos \lambda t + B\sin \lambda t$.

Lemma 3 – *The minimum value of $\int u_t^2 + \lambda^2 u^2 \mathrm{d}t$ on an interval of length T with boundary values $u(0) = b$ and $u(T) = c$ is*

$$\lambda((b^2 + c^2)\cosh(\lambda T) - 2bc)/\sinh(\lambda T) \quad (6)$$

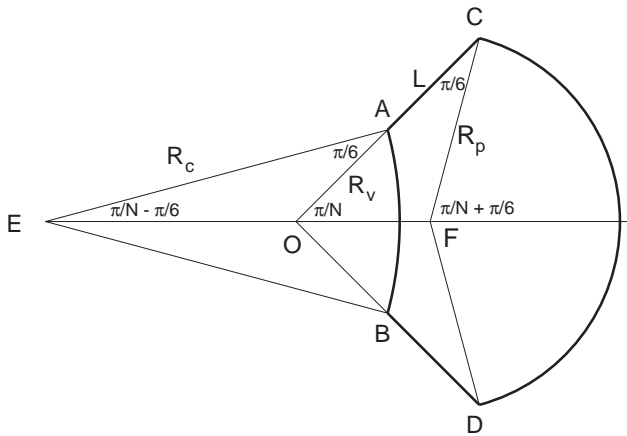*and occurs when $u(t)$ is of the form $u(t) = A\cosh \lambda t + B\sinh \lambda t$.*
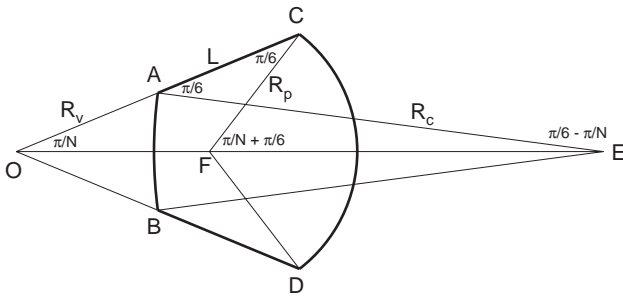
Fig. 3. Petal geometry, $N < 6$.

Fig. 4. Petal geometry, $N > 6$.

3 Notation

We use the following notation in Sections 4-9 (see Figs. 3, 4):

N number of petals (outer bubbles),
H height; cluster is bounded by planes
     $z = -H/2$ and $z = H/2$,
R_v radius of inner triple junction from central axis,
R_p radius of outer surface,
R_c radius of inner surface,
L length of septum (wall between petals),
V_c volume of central bubble,
V_p volume of petal bubble,
σ^2 sum of squares of principal curvatures,
T_i length of inner arc,
T_o length of outer arc,
u normal component of variation vector field,
s u on septa at inner vertex,
t local arclength parameter.

4 Geometry

This section lays out the basic geometry of a cylindrical bubble cluster of N identical petals surrounding a central bubble as in Figure 1. The assumption of cylindrical form means that all surfaces are either planes or circular cylinders. The pressure change across a surface is proportional to its curvature. Since the petals are identical, the walls, or *septa*, between the petals are planes.

We will consider clusters with three or more petals. A cluster with two petals is in equilibrium, but it is only metastable, since the central bubble can drift out along the coplanar septa and re-arrange into a lower-energy configuration when it touches the outer surfaces.

The geometry for $N < 6$ is given by the following formulas (Fig. 3). The equations are valid also for $N > 6$, with R_c negative (Fig. 4).

The inner cell area, OAB:

$$R_c^2\left(\frac{\pi}{N} - \frac{\pi}{6}\right) - R_v R_c \sin\frac{\pi}{6} = \frac{1}{H}\frac{V_c}{N}. \tag{7}$$

Length relations from the Law of Sines:

$$\frac{R_c}{\sin\frac{\pi}{N}} = \frac{R_v}{\sin\left(\frac{\pi}{N} - \frac{\pi}{6}\right)}, \tag{8}$$

providing an equation solvable for R_c and thence R_v:

$$R_c^2\left(\frac{\pi}{N} - \frac{\pi}{6}\right) - R_c^2\frac{\sin\left(\frac{\pi}{N} - \frac{\pi}{6}\right)}{\sin\frac{\pi}{N}}\sin\frac{\pi}{6} = \frac{1}{H}\frac{V_c}{N}, \tag{9}$$

except that when $N = 6$:

$$R_c = \infty, \qquad R_v^2\sin\frac{\pi}{6}\cos\frac{\pi}{6} = \frac{1}{H}\frac{V_c}{N}. \tag{10}$$

The outer cell area, ABDC:

$$R_p^2\left(\frac{\pi}{N} + \frac{\pi}{6}\right) + (R_v + L)R_p\sin\frac{\pi}{6} - \frac{1}{H}\frac{V_c}{N} = \frac{1}{H}V_p. \tag{11}$$

Length relations from the Law of Sines:

$$\frac{R_p}{\sin\frac{\pi}{N}} = \frac{R_v + L}{\sin\left(\frac{\pi}{N} + \frac{\pi}{6}\right)}, \tag{12}$$

providing an equation solvable for R_p and thence L:

$$R_p^2\left(\frac{\pi}{N} + \frac{\pi}{6}\right) + R_p^2\frac{\sin\left(\frac{\pi}{N} + \frac{\pi}{6}\right)}{\sin\frac{\pi}{N}}\sin\frac{\pi}{6} - \frac{1}{H}\frac{V_c}{N} = \frac{1}{H}V_p. \tag{13}$$

5 Petal Rayleigh mode

The petal Rayleigh mode is antisymmetric in z, with N petals (N even) alternately bulging at top or bottom. Due to the antisymmetry in z, volume preservation is assured. Surface Evolver simulations show that the lowest eigenmode has multiplicity one, and therefore the eigenvector must share the D_N symmetry (rotational and reflectional) of the cluster.

Theorem 3 – *For even N, the second variation of petal Rayleigh mode can be expressed in closed form as a function of N, V_c, V_p, and H, given by the sum of contributions (17,19,21,25,27,29,30), with critical heights partially tabulated in Table 2.*

Table 2. Petal Rayleigh mode critical heights for various numbers of petals and various central volumes. The petal volume is 1.

N	$V_c = 0.5$	$V_c = 1.0$	$V_c = 1.5$
4	1.79655	1.82512	1.85534
6	1.77121	1.78948	1.80816
8	1.70967	1.73929	1.75815
10	1.56989	1.66913	1.70135

Proof: The second variation will be calculated for one fundamental region of the cluster consisting of one septum, one inner wall, and one outer wall. By separation of variables, we will take the normal component u of the perturbation to be of the form

$$u = v(t)w(z). \tag{14}$$

The second variation (Eq. (3)) becomes

$$\delta^2 A = \int \int v_t^2 w^2 + v^2 w_z^2 - \sigma^2 v^2 w^2 \mathrm{d}t \, \mathrm{d}z$$
$$- \sum_j \int_{C_j} \sum_{i=1}^3 q_i v_i^2 w^2 \mathrm{d}z,$$

which can be rewritten as

$$\delta^2 A = \int_{-H/2}^{H/2} \left[\int v^2 \mathrm{d}t \right] w_z^2$$
$$+ \left[\int v_t^2 - \sigma^2 v^2 w^2 \mathrm{d}t - \sum_{C_j} \sum_{i=1}^3 q_i v_i^2 \right] w^2 \mathrm{d}z.$$

For $\delta^2 A$ to be zero, the coefficient of w^2 must be negative, so the antisymmetry of $w(z)$ and *Lemma 2* tell us that the second variation is minimized when $w(z)$ is of the form

$$w(z) = \sin \frac{\pi z}{H}. \tag{15}$$

The second variation with z integrated out is

$$\delta^2 A = \int \frac{H}{2} v_t^2 + \frac{\pi^2}{2H} v^2 - \frac{H}{2}\sigma^2 v^2 \mathrm{d}t - \frac{H}{2}\Sigma_i q_i v_i^2. \tag{16}$$

On a septum the curvature is zero, so we want to minimize

$$\delta^2 A_{\text{septum}} = \int \frac{H}{2} v_t^2 + \frac{\pi^2}{2H} v^2 \mathrm{d}t$$
$$= \frac{H}{2} \int v_t^2 + \frac{\pi^2}{H^2} v^2 \mathrm{d}t,$$

over a segment of length L with boundary conditions $v(0) = s$ and $v(L) = 1$. By *Lemma 3* the minimal value is

$$\delta^2 A_{\text{septum}} = \frac{H}{2} \frac{\pi}{H} \left((1 + s^2) \cosh \frac{\pi L}{H} - 2s \right) \Big/ \sinh \frac{\pi L}{H}. \tag{17}$$

On the inner arc the curvature is $1/R_c$, so we want to minimize

$$\delta^2 A_{\text{inner}} = \int \frac{H}{2} v_t^2 + \frac{\pi^2}{2H} v^2 - \frac{H}{2} \frac{1}{R_c^2} v^2 \mathrm{d}t$$
$$= \frac{H}{2} \int v_t^2 + \left(\frac{\pi^2}{H^2} - \frac{1}{R_c^2} \right) v^2 \mathrm{d}t,$$

over a segment of length

$$T_i = 2R_c \left(\frac{\pi}{N} - \frac{\pi}{6} \right) \tag{18}$$

with boundary conditions $v(0) = s/2$ and $v(T_i) = s/2$. By *Lemma 3* the minimal value is

$$\delta^2 A_{\text{inner}} = \frac{H}{2} \frac{s^2}{2} \lambda_i ((\cosh(\lambda_i T_i) - 1) / \sinh(\lambda_i T_i), \tag{19}$$

where

$$\lambda_i = \sqrt{\frac{\pi^2}{H^2} - \frac{1}{R_c^2}}. \tag{20}$$

Technically, this still works if λ_i turns out imaginary; in that case we can stay real with *Lemma 2* and

$$\delta^2 A_{\text{inner}} = \frac{H}{2} \frac{s^2}{2} \lambda_i ((\cos(\lambda_i T_i) - 1) / \sin(\lambda_i T_i), \tag{21}$$

where

$$\lambda_i = \sqrt{\frac{1}{R_c^2} - \frac{\pi^2}{H^2}}. \tag{22}$$

For the special case of $N = 6$,

$$T_i = R_v/2 \tag{23}$$

with other formulas the same.

On the outer arc, the curvature is $1/R_p$, so we want to minimize

$$\delta^2 A_{\text{outer}} = \int \frac{H}{2} v_t^2 + \frac{\pi^2}{2H} v^2 - \frac{H}{2} \frac{1}{R_p^2} v^2 \mathrm{d}t$$
$$= \frac{H}{2} \int v_t^2 + \left(\frac{\pi^2}{H^2} - \frac{1}{R_p^2} \right) v^2 \mathrm{d}t,$$

over a segment of length

$$T_o = 2R_p \left(\frac{\pi}{N} + \frac{\pi}{6} \right), \tag{24}$$

with boundary conditions $v(0) = 1/2$ and $v(T_o) = 1/2$. By *Lemma 3* the minimal value is

$$\delta^2 A_{\text{outer}} = \frac{H}{2} \frac{1}{2} \lambda_o (\cosh(\lambda_o T_o) - 1) / \sinh(\lambda_o T_o), \tag{25}$$

where

$$\lambda_o = \sqrt{\frac{\pi^2}{H^2} - \frac{1}{R_p^2}}, \tag{26}$$

or

$$\delta^2 A_{\text{outer}} = \frac{H}{2} \frac{1}{2} \lambda_o (\cos(\lambda_o T_o) - 1) / \sin(\lambda_o T_o), \tag{27}$$

where

$$\lambda_{\mathrm{o}} = \sqrt{\frac{1}{R_{\mathrm{p}}^2} - \frac{\pi^2}{H^2}}. \tag{28}$$

For the triple junctions, the contribution for the inner triple junction is

$$\delta^2 A_{\mathrm{itriple}} = -\frac{H}{2}\frac{1}{\sqrt{3}}\left[-\left(\frac{1}{R_{\mathrm{c}}} + \frac{1}{R_{\mathrm{c}}}\right)s^2 + \frac{1}{R_{\mathrm{c}}}\left(\frac{s}{2}\right)^2 + \frac{1}{R_{\mathrm{c}}}\left(\frac{s}{2}\right)^2\right],$$

or

$$\delta^2 A_{\mathrm{itriple}} = \frac{\sqrt{3}s^2 H}{4R_{\mathrm{c}}}. \tag{29}$$

The contribution for the outer triple junction is

$$\delta^2 A_{\mathrm{otriple}} = -\frac{H}{2}\frac{1}{\sqrt{3}}\left[\left(\frac{1}{R_{\mathrm{p}}} + \frac{1}{R_{\mathrm{p}}}\right)1^2 - \frac{1}{R_{\mathrm{p}}}\left(\frac{1}{2}\right)^2 - \frac{1}{R_{\mathrm{p}}}\left(\frac{1}{2}\right)^2\right],$$

or

$$\delta^2 A_{\mathrm{otriple}} = -\frac{\sqrt{3}H}{4R_{\mathrm{p}}}. \tag{30}$$

$$\square$$

Remark 3 – If there are an odd number of petals, the petal Rayleigh mode is frustrated. Instead, the low mode is the petal Rayleigh mode modulated by a $\sin\theta/2$ factor, so that in going once around, the sign of the perturbation makes a change, in addition to the sign changes in going from petal to petal. It turns out that the phase of the modulation is irrelevant, so the eigenspace is two dimensional. This means that individual eigenvectors do not have to share the D_N symmetry of the cluster, which considerably complicates the analysis. A future paper will address this case and the case of general clusters.

Remark 4 – Answering a question of R. Kusner, for clusters with outer radius of curvature R_{p}, the critical height is sometimes less and sometimes greater than πR_{p}, the value suggested by a single bubble.

6 Petal buckling mode

As a cylinder, the cluster inherits all the eigenmodes of its two-dimensional cross-section. Clearly, instability here is independent of height, and simply depends on the bubble size ratios. These "buckling" modes, as in Figure 5, were studied by Weaire, Cox, and Graner [9], with the conclusion that instability sets in when the pressure in the central bubble becomes negative, which can happen only for $N \geq 7$. The reason is very simple: when the central pressure is zero, the inner and outer radii are of the same magnitude and each petal is a section of a disk. Adjacent petals can slide along one another without changing their
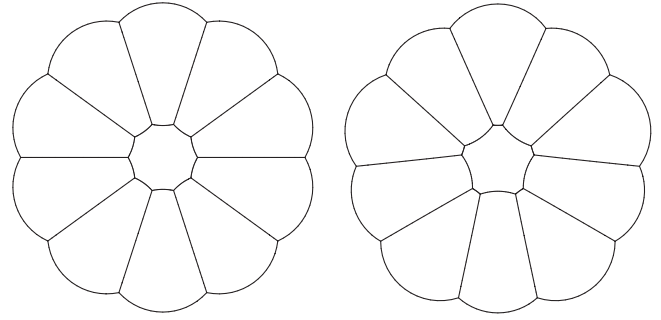

Fig. 5. Symmetric but unstable ten-petal cluster and one of the possible buckling modes.

Table 3. Petal buckling mode critical central volumes V_{c} for petal volume $V_{\mathrm{p}} = 1$ and various number of petals. The cluster is unstable for smaller values of V_{c}. Also listed is the petal Rayleigh mode critical height.

N	Critical V_{c}	Petal Rayleigh critical height
7	0.04141	1.62029
8	0.16576	1.62099
9	0.37315	1.62146
10	0.66364	1.62180
11	1.03726	1.62205
12	1.49403	1.62223
13	2.03396	1.62238
14	2.65705	1.62249
20	8.14234	1.62286

circularity, so disregarding the central-volume constraint, the ring of petals acts as a flexible string of beads. By counting degrees of freedom, one sees that there are $N-3$ modes of deformation (besides translation and rotation), which are thus zero-eigenvalue modes of the petal ring. These modes all preserve the central area to first order, and since adding a constraint which is already satisfied does not change eigenvalues of eigenmodes that preserve that constraint, all the $N-3$ modes have zero eigenvalue with the central-area constraint. When the central pressure is not zero, positive central pressure keeps the petal ring stretched out in a circle, and negative central pressure sucks some petals toward the center.

Theorem 4 – *(Ref. [9], Eq. (2)) A cylindrical cluster of $N \geq 7$ identical petals of volume V_{p} surrounding a central bubble of volume V_{c} has buckling instability if the volume ratio exceeds the critical ratio,*

$$\frac{V_{\mathrm{c}}}{V_{\mathrm{p}}} = \left(\frac{1}{3} + \frac{\sqrt{3}}{2\pi}\right)\left[\frac{N}{2\pi}\frac{\sin(\pi/6 - \pi/N)}{\sin(\pi/N)} + 1 - \frac{N}{6}\right]. \tag{31}$$

The critical central volume values are shown in Table 3, along with the petal Rayleigh critical height for petal volume 1. The petal Rayleigh critical heights are remarkably uniform. If the cylindrical beads were in a straight line, then the petal Rayleigh instability would be independent of N. Apparently, the petal Rayleigh instability of a string

Table 4. Critical heights for central Rayleigh instability. Note that these are independent of the petal volume.

N	Central Rayleigh critical height, $\times V_\mathrm{c}^{1/3}$
3	1.84681
4	2.11270
5	2.66141
6	∞

of cylindrical beads is very little affected by bending by various degrees around the central bubble.

7 Central Rayleigh mode

In the central Rayleigh instability, the top of the central bubble bulges out, and the bottom pinches in. The petals are otherwise unaffected. It occurs only for $N < 6$, when the central bubble bulges out.

Theorem 5 – *The second variation of the central Rayleigh mode can be expressed in closed form as a function of N and V_c, given by the sum of contributions (19) or (21) with $s = 2$ and (35), with critical heights partially tabulated in Table 4.*

Proof: The second variation of

$$u = v(t) \sin \frac{\pi z}{H} \tag{32}$$

with z integrated out becomes

$$\delta^2 A = \int \frac{H}{2} v_t^2 + \frac{\pi^2}{2H} v^2 - \frac{H}{2} \sigma^2 v^2 \mathrm{d}t - \frac{H}{2} \Sigma_i q_i v_i^2. \tag{33}$$

On each septum, v is zero. On the inner arc, everything is the same as in the even petal Rayleigh mode, except that v is 1 at the ends instead of $s/2$, so we can use the petal Rayleigh $\delta^2 A_\mathrm{inner}$ with $s = 2$. On the outer arc v is zero. The contribution for the inner triple junction is

$$\delta^2 A_\mathrm{itriple} = -\frac{H}{2} \frac{1}{\sqrt{3}} \left[-\left(\frac{1}{R_\mathrm{c}} + \frac{1}{R_\mathrm{c}} \right) 0^2 + \frac{1}{R_\mathrm{c}} 1^2 + \frac{1}{R_\mathrm{c}} 1^2 \right] \tag{34}$$

or

$$\delta^2 A_\mathrm{itriple} = -\frac{H}{\sqrt{3} R_\mathrm{c}}. \tag{35}$$

The contribution for the outer triple junction is zero. □

8 Two-bubble cluster

None of the configurations discussed so far include the simple case of two adjacent bubbles. We will just do the equal-volume case here for simplicity, to fill in row (b) of Table 1.

Theorem 6 – *The cluster of two adjoining identical bubbles becomes unstable petal Rayleigh mode at a critical height of approximately* 1.51906.

Proof: For bubble volume 1, the bubble radius is

$$R = \left[H \left(\frac{\sqrt{3}}{4} + \frac{2\pi}{3} \right) \right]^{-1/2} \tag{36}$$

and the arc length of one bubble is

$$T = \frac{4\pi}{3} R. \tag{37}$$

Take the perturbation $u = u(t) \sin(\pi z / H)$ to have $u(t) = 1$ on the septum ends and magnitude $1/2$ at the ends of the arcs. Working out the septum, arc, and triple junction variations as before gives

$$\delta^2 A = \frac{\pi \cosh(\pi\sqrt{3}R/H)}{\sinh(\pi\sqrt{3}R/H)} + \frac{H}{2} \frac{\lambda(\cosh(\lambda T) - 1)}{\sinh(\lambda T)} - \frac{\sqrt{3}}{2} \frac{H}{R}, \tag{38}$$

where

$$\lambda^2 = \frac{\pi^2}{H^2} - \frac{1}{R^2}. \tag{39}$$

The critical height is

$$H \approx 1.51906. \tag{40}$$

□

As a point of interest, the mode where both bubbles expand at the top and shrink at the bottom turns out to have a critical height of 1.69146.

9 Surface Evolver simulations

To verify the accuracy of these theoretical calculations and to check that no instability modes were overlooked, Surface Evolver simulations of various configurations were carried out. The Surface Evolver [6] is freely available software that is models energy minimization problems involving triangulated surfaces, and it is capable of calculating eigenvalues numerically and displaying eigenmodes. However, calculating eigenmodes with the full three degrees of freedom at each unconstrained vertex of the triangulation yields many near-zero eigenvalues that involve shifting the triangulation around laterally rather than the modes we seek. Therefore, the Evolver can constrain the degrees of freedom. The default mode, called Hessian normal mode, constrains each vertex to move normal to the surface, except that vertices on triple junctions have two degrees of freedom perpendicular to the triple junction and tetrahedral points keep the full three degrees of freedom. It is also possible to explicitly set the direction of motion allowed for each vertex, in what is called Hessian special normal mode. It is also possible to put on constraints that suppress the trivial eigenmodes of translation and rotation.

There are two issues to check: first, whether the critical heights calculated for the modes are in fact accurate, and second, whether any modes of instability have been missed. For the first issue, Hessian special normal mode was used with the direction being that assumed for petal Rayleigh mode. Simulations of 4, 6, 8, and 10 petals at petal volume 1 and central volumes 0.5, 1.0, 1.5, 2.0, 3.0, and 4.0 at the critical heights showed the lowest eigenvalues to be less than 3×10^{-6} in magnitude. For the second issue, the default Hessian normal mode was used, since it does not prejudge the nature of the mode. However, it is considerably less accurate in evaluating individual eigenvalues due to modes distorting the triangulation around triple junctions. But it did show that the predicted modes were the lowest eigenvalues by a comfortable margin for the cases tested. Simulation of the double-bubble cluster similarly confirmed predictions.

10 Conclusions

Cylindrical clusters of N petals around a central bubble well illustrate two prototypical three-dimensional Rayleigh-Plateau instabilities in two-dimensional clusters, "central" and "petal" Rayleigh-Plateau instabilities. When the central bubble is small and has fewer than six sides, it becomes unstable first. When it is large or has six or more sides, the petal instability occurs first. In general, the first Rayleigh-Plateau instabilities occur with smaller, convex bubbles of few sides. There are many other interesting clusters that could be analyzed, such as the energy-minimizing clusters of four or more equal-volume planar bubbles. For large, disordered clusters of cylindrical bubbles, as in typical two-dimensional foams, we likewise expect that instability begins with small, high-pressure, few-sided bubbles. In further work, we intend to analyze the instabilities in such general clusters, and develop an understanding of the role of disorder.

It should be possible to analyze the stability of general cylindrical clusters systematically. Careful examination of the second variation expressions show they are quadratic functions of the perturbations at the triple junctions, so the critical height problem can be reduced to determining when a quadratic form depending on H becomes indefinite. Work is underway to implement this scheme in a computer program.

References

1. S.J. Cox, D. Weaire, M.F. Vaz, Eur. Phys. J. E **7**, 311 (2002).
2. M. Athanassenas, J. Reine Ang. Math. **377**, 97 (1987).
3. T.I. Vogel, SIAM J. Appl. Math. **47**, 516 (1987).
4. M. Hutchings, F. Morgan, M. Ritoré, A. Ros, Ann. Math. **155**, 459 (2002), http://www.ugr.es/~ritore/bubble/bubble.htm.
5. *Mathematica*, Wolfram Research, Inc.
6. K.A. Brakke, Exper. Math. **1**, 141 (1992).
7. F. Morgan, *Geometric Measure Theory: a Beginner's Guide*, third edition (Academic Press, 2000).
8. F. Morgan, M. Ritoré, Trans. AMS **354**, 2327 (2002), http://www.ugr.es/~ritore/preprints/cone.pdf.
9. D. Weaire, S. Cox, F. Graner, Eur. Phys. J. E **7**, 123 (2002).